

Thermochemical Study of Theophylline and Its Hydrate

Etsuko SUZUKI,* Kikuko SHIMOMURA, and Keiji SEKIGUCHI

School of Pharmaceutical Sciences, Kitasato University, 9-1, Shirokane 5-chome, Minato-ku, Tokyo 108, Japan. Received August 3, 1988

Anhydrous theophylline exhibited polymorphism and two modifications, which were named form I and form II, were isolated. The melting point and the enthalpy of fusion of each polymorph determined by differential scanning calorimetry (DSC) were $273.4 \pm 1.0^\circ\text{C}$ and $26.4 \pm 0.3 \text{ kJ/mol}$ for form I and $269.1 \pm 0.4^\circ\text{C}$ and $28.2 \pm 1.1 \text{ kJ/mol}$ for form II. The higher melting form I had a smaller density. In contrast to caffeine, theophylline formed a monohydrate. The dissociation vapor pressure curves of theophylline hydrate and caffeine hydrate were obtained and the difference in their stabilities was discussed. The enthalpy of dehydration was determined by DSC under closed conditions. The dehydration under isothermal conditions appeared to proceed according to the mechanism of random nucleation followed by two-dimensional growth of nuclei as represented by the Avrami-Erofe'ev equation. The solubilities of theophylline and its hydrate were determined as a function of temperature. From the van't Hoff type plot, the transition temperature between the hydrate and the anhydrous form was determined.

Keywords anhydrous theophylline; theophylline hydrate; polymorph; dehydration kinetics; dissociation vapor pressure; dissolution behavior

In our preceding paper,¹⁾ the water content and the dehydration behavior of crystalline caffeine hydrate were discussed. This study indicated that anhydrous caffeine exists in two polymorphic forms and the stable hydrate contains 0.8 mol of water per mol of caffeine.

It is well-known that theophylline, another xanthine derivative, is capable of existing in anhydrous or hydrous form. The present paper deals with theophylline and its hydrate. Although Bruns *et al.* could not find the evidence for a polymorphic transition of anhydrous theophylline,²⁾ Burger and Ramberger have preliminarily reported the presence of polymorphs.³⁾ Since details remain obscure, the isolation of the polymorphs was attempted. The polymorphs were characterized by means of differential scanning calorimetry, X-ray powder diffractometry and so forth. The thermochemical properties of the hydrate were studied by water vapor pressure measurements and isothermal thermogravimetry.

Experimental

Materials The preparation of caffeine hydrate has been previously described in detail.¹⁾ Theophylline hydrate was prepared in the same way as caffeine hydrate. It was quite stable on storage at 97% relative humidity over a saturated solution of calcium sulfate. The hydrate was converted to an anhydrous form under a given temperature and reduced pressure.

Differential Scanning Calorimetry (DSC) An SSC 580/DSC 20 differential scanning calorimeter (Seiko Instruments Inc.) was used. Gas-tight (hermetic) containers which could withstand a pressure of 50 atm were used for the measurements under closed conditions. The DSC apparatus was calibrated with distilled water, indium, and tin. Samples were run at a scanning rate of 1 or 5°C/min using dry nitrogen as the effluent gas.

Infrared (IR) Spectroscopy IR spectra were measured by the Nujol mull method using a Jasco IRA-1 grating infrared spectrophotometer.

X-Ray Powder Diffractometry X-Ray diffraction patterns were obtained using a JEOL JDX-7F X-ray diffraction analyzer with Ni-filtered $\text{CuK}\alpha$ radiation ($\lambda = 1.542 \text{ \AA}$).

Scanning Electron Microscopy A MINI SEM model MSM-4 was used (Hitachi-Akashi Co., Ltd.).

Thermomicroscopy The dehydration process of theophylline hydrate was observed microscopically with Mettler FP 5 and FP 52 apparatus.

Measurements of Specific Surface Area and Water Vapor Pressure The specific surface area and the dissociation vapor pressure were measured using a BET gas adsorption and water vapor sorption apparatus (model P-850, Shibata Scientific Technology, Ltd.). The vapor pressure of the hydrate at $25\text{--}40^\circ\text{C}$ was determined by a static method using a mercury

manometer.

Isothermal Thermogravimetry (TG) A Thermoflex TG-DSC apparatus (Rigaku Denki Co., Ltd.) was used. Theophylline hydrate with no trituration was sieved and crystals of 100—200 mesh size were used. About 10 mg of sample, weighed precisely, was employed in every run. The atmosphere was dry nitrogen, which was regulated at a constant flow of 10 ml/min.

Dissolution Experiments A quantity of sample powder (50—100 mesh) in excess of its solubility was weighed and rapidly introduced into a 200 ml water-jacketed cell containing exactly 100 ml of distilled water maintained at a constant temperature. The solution was stirred with a Teflon-covered magnetic stirring bar at 600 rpm. At suitable intervals, aliquots of the solution were withdrawn, filtered through Millipore membrane filter paper (pore size $0.45 \mu\text{m}$), and immediately diluted with an appropriate amount of distilled water. Theophylline was analyzed at 272 nm with a Shimadzu UV-200 double-beam spectrophotometer.

Results and Discussion

DSC, X-Ray Diffraction, and IR Spectra of Anhydrous Theophylline We have noticed that among anhydrous theophylline preparations, there were several samples for which the DSC melting peak tops were separated into two peaks. In those samples, the peak separation became greater at decreasing heating rates. As this phenomenon was presumably attributable to polymorphism, isolation of

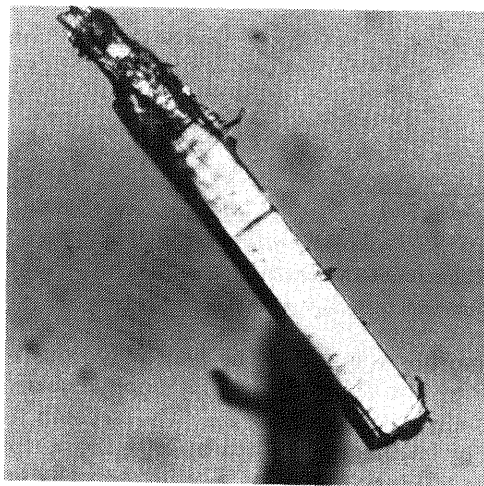


Fig. 1. Photomicrograph of Anhydrous Theophylline Form I ($60\times$)

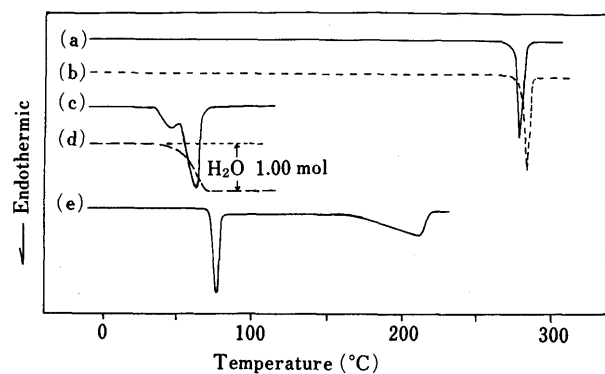


Fig. 2. DSC and TG Curves of Theophylline (Heating Rate: 1 °C/min)

(a) DSC curve of anhydrous form II under closed conditions. (b) DSC curve of anhydrous form I under closed conditions. (c) DSC curve of hydrate under open conditions. (d) TG curve of hydrate. (e) DSC curve of hydrate under closed conditions.

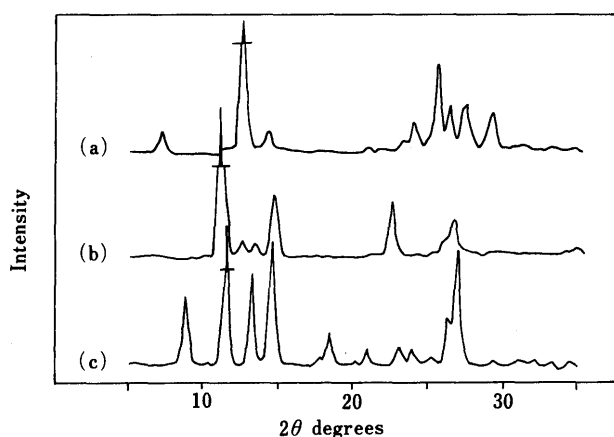


Fig. 3. X-Ray Powder Diffraction Patterns of Theophylline

(a) Anhydrous form II. (b) Anhydrous form I. (c) Hydrate.

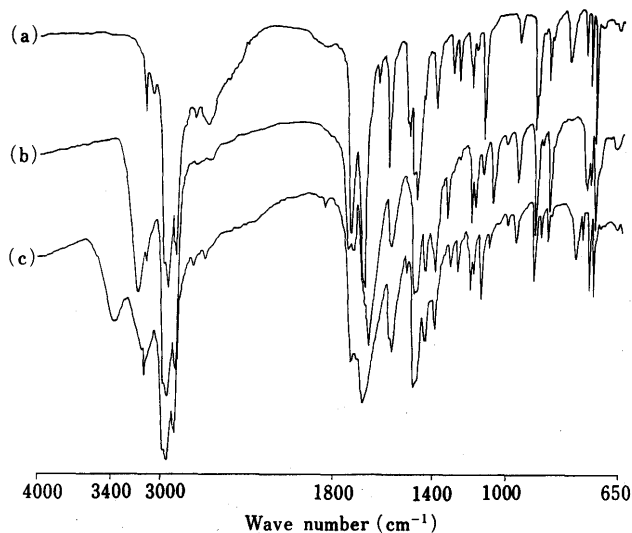


Fig. 4. IR Spectra of Theophylline (Nujol Mull)

(a) Anhydrous form II. (b) Anhydrous form I. (c) Hydrate.

the polymorphs was tried. The first anhydrous form was prepared by the dehydration of theophylline hydrate at 110 °C under reduced pressure. The second form was obtained by heating the first one at 260–268 °C for 1 h in a thick glass test tube which could be hermetically sealed. We designated the first as form II and the second as form I.

TABLE I. Thermal Data of Theophylline

Transition	Temperature (°C)	Enthalpy change (kJ/mol)
Anhydrous form II→liquid	269.1 ± 0.4	28.2 ± 1.1
Anhydrous form I→liquid	273.4 ± 1.0	26.4 ± 0.3
Hydrate→anhydrous form II	71.0 ± 0.9	10.6 ± 0.1

DSC measurements were carried out under closed conditions (heating rate: 1 °C/min).

TABLE II. Density Data of Theophylline at 24 °C

Crystal form	Density (g/ml)
Anhydrous form II ^{a)}	1.502
Anhydrous form I	1.489
Hydrate	1.453

a) Recrystallized from methanol.

Figure 1 is a photomicrograph of anhydrous form I. Both of the anhydrous forms had only one endothermic peak on each DSC curve as shown in Fig. 2(a) and (b).

Their X-ray powder diffraction patterns and IR spectra are in Fig. 3(a) and (b), and Fig. 4(a) and (b). Elemental analysis (C, H, N, O) of the two anhydrous forms coincided with the theoretical values within the experimental errors. Mass spectra (MS) were also identical with the literature data.⁴⁾ Thus, melting points, X-ray powder diffraction patterns, and IR spectra of the two anhydrous forms were different, while their elemental analysis and MS agreed very well with each other. From these results it was considered that the two kinds of anhydrous theophylline were polymorphs. The thermal data obtained from DSC measurements under closed conditions are given in Table I. When heating the anhydrous form II on a hot stage, tabular or needle-like crystals appeared gradually near 245 °C. Doser has observed microscopically that a polymorphic transition occurs near 260 °C.⁵⁾ Nevertheless, no solid–solid phase transition could be detected on our DSC curve. While the enthalpy of transition may be very small, further investigation is needed.

The densities of the crystals, determined by the floating method in a carbon tetrachloride–cyclohexane mixture, are shown in Table II. Sutor reported that the density of the hydrate is 1.452,⁶⁾ which is consistent with our data. Wadke and Reier reported that the densities of the hydrate and the anhydrous form are 1.52 and 1.44, respectively.⁷⁾ The reason why the value of the anhydrous form is small compared with our value would be because they used the anhydrous form prepared by heating the monohydrate at 100 °C. Tables I and II indicate that the higher melting form I has a lower heat of fusion and a smaller density.

DSC, X-Ray Diffraction, and IR Spectra of Theophylline Hydrate Figure 2(c) shows the DSC pattern of theophylline hydrate under open conditions. A broad endothermic peak around 35–70 °C is due to the dehydration and the subsequent evaporation of water. The TG curve corresponding to the DSC curve (c) is (d). The weight decrease is equivalent to 1.00 mol of water. Curve (e) is the DSC pattern under closed conditions. The first peak near 71 °C is ascribed to the peritectic reaction of the hydrate and the

peak onset decreases with decreasing heating rate as pointed out by Bruns *et al.*²⁾ The second peak at about 215 °C is due to the melting of solid theophylline. The enthalpy of dehydration determined from the peak area is shown in Table I. Since the heat of evaporation of water measured under the same conditions was 37.5 kJ/mol, this value (10.6 ± 0.1 kJ/mol) was almost equal to the value obtained by subtracting the heat of evaporation of water from the heat value corresponding to the whole area of the DSC curve (c) (47.6 kJ/mol).

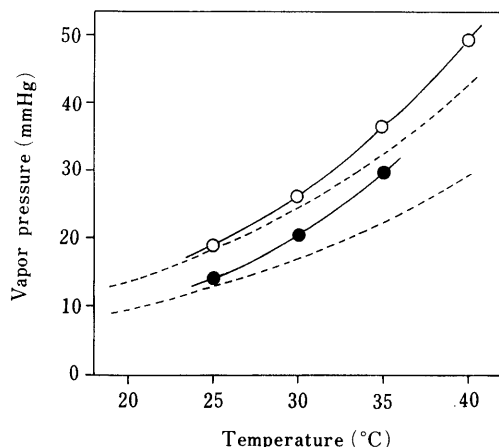


Fig. 5. Vapor Pressure-Temperature Curves of Theophylline Hydrate and Caffeine Hydrate

●, theophylline hydrate; ○, caffeine hydrate. The dotted curves represent the normal maximum and minimum relative humidities (upper, 77%; lower, 53%).

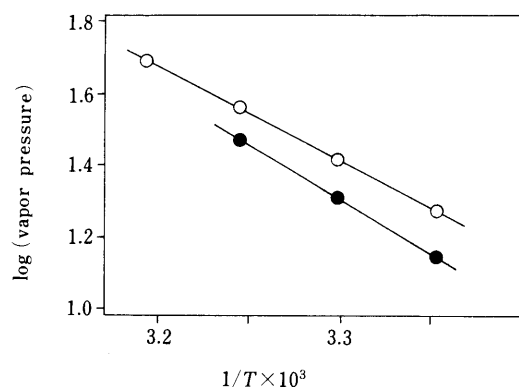


Fig. 6. $\log(\text{vapor pressure}) - 1/T$ Curves of Theophylline Hydrate and Caffeine Hydrate

●, theophylline hydrate; ○, caffeine hydrate.

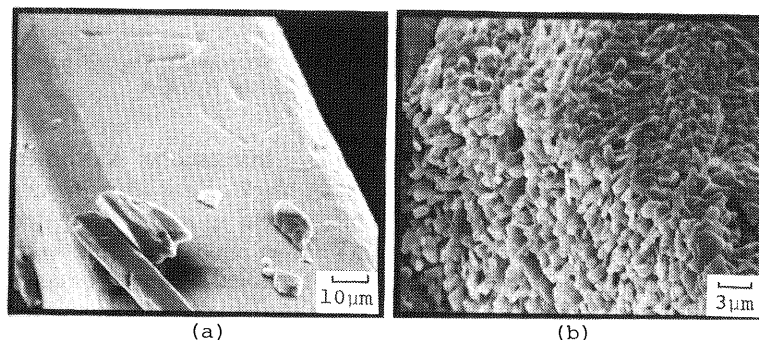


Fig. 7. Scanning Electron Micrographs of Theophylline

(a) Theophylline hydrate, 1000 ×. (b) Theophylline after dehydration, 3000 ×.

The X-ray powder diffraction pattern and the IR spectrum are shown in Fig. 3(c) and Fig. 4(c). The IR spectrum shows a broad absorption around 3400 cm^{-1} owing to the hydrogen bond between N_6 of the theophylline molecule and a water molecule in addition to the hydrogen bonds among water molecules.⁶⁾

Water Vapor Pressure of Theophylline Hydrate Figure 5 shows the dissociation vapor pressure curves of theophylline hydrate and caffeine hydrate. The dotted curves represent the normal maximum and minimum relative humidities classified by months⁸⁾ in Tokyo, *i.e.*, 77% in July and 53% in January.⁹⁾ From Fig. 5, it can be seen that at atmospheric pressure caffeine hydrate has a tendency to transform exclusively to the anhydrous form, but theophylline should change form reversibly according to the atmospheric moisture content. A plot of $\log(\text{vapor pressure})$ versus the reciprocal of absolute temperature gives a straight line as shown in Fig. 6. The heat of dissociation calculated from the slope of this line was 57.5 kJ/mol, and is appreciably larger than the value determined from DSC (47.6 kJ/mol). The heat of dissociation of caffeine hydrate was reported in the preceding paper.¹⁾

It seems likely that the repeated hydration and dehydration during storage may result in changes of particle shapes and sizes of theophylline. As shown in electron micrographs of Fig. 7, the surface of the hydrate is smooth, while the anhydrous form, in spite of retaining the original external shapes, consists of agglomerates of smaller particles.

In order to study such alterations in crystal appearance quantitatively, the specific surface areas were determined. Although the actual reactions proceed under mild conditions, namely at room temperature and 1 atm, rather extreme conditions as below were adopted. That is to say, the hydrate was converted into the anhydrous form at room temperature and reduced pressure, whereas the anhydrous form was returned into the hydrate on standing at room temperature and 97% relative humidity. The changes of specific surface area caused by the repetition of three hydration-dehydration cycles are shown in Table III. The elimination of the water of crystallization from the original hydrate resulted in a seven-fold increase in the specific surface area, but further repetition did not bring about any additional increase under such experimental conditions. This may be ascribed to particle bridging due to liquid formation (*e.g.* capillary condensation and saturated water layers on the crystal surface) during the hydration

TABLE III. Changes of Specific Surface Area by Repeated Hydration and Dehydration of Theophylline

Sample	Specific surface area (m ² /g)
First cycle	
Hydrate	0.22
Anhydrous	1.46
Second cycle	
Hydrate	0.22
Anhydrous	2.22
Third cycle	
Hydrate	0.27
Anhydrous	1.35

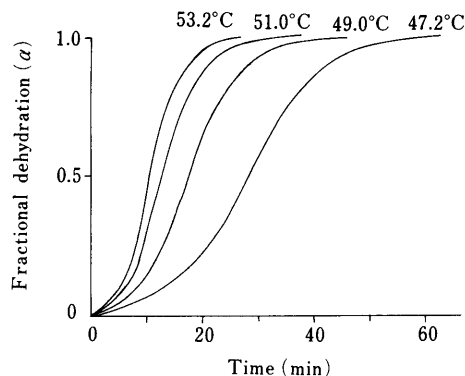
Fig. 8. Isothermal α -Time Curves for the Dehydration of Theophylline Hydrate

TABLE IV. Solid-State Reaction Rate Equations to Which Obedience of Isothermal Dehydration Data was Tested

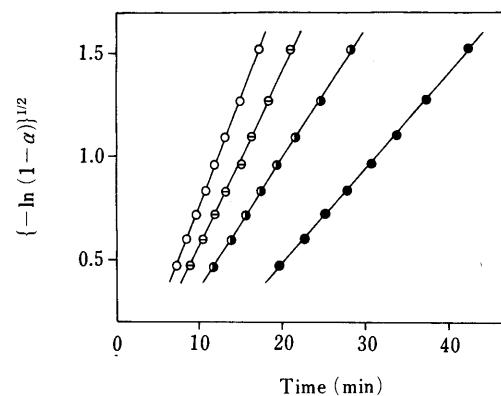
Equation ^{a)}	Label
Sigmoid rate equations	
Avrami-Erofe'ev $\{-\ln(1-\alpha)\}^{1/2} = kt$	A ₂
$\{-\ln(1-\alpha)\}^{1/3} = kt$	A ₃
Deceleratory rate equations	
Phase boundary-controlled reaction	
Contracting area $1 - (1-\alpha)^{1/2} = kt$	R ₂
Contracting volume $1 - (1-\alpha)^{1/3} = kt$	R ₃
First order $-\ln(1-\alpha) = kt$	F ₁

a) Times are assumed to have been corrected for any induction period.

processes.

Dehydration Mechanism of Theophylline Hydrate Figure 8 shows the fractional dehydration (α)-time plots for the isothermal dehydration of theophylline hydrate. Throughout the reaction period except at $\alpha < 0.1$, the temperature was kept satisfactorily constant. The kinetic obedience to various rate equations which have found the greatest application in solid-phase reactions was investigated. Table IV summarizes the functional relationship between α and time, namely $f(\alpha) = kt$, where k is the reaction rate constant and t is the time.¹⁰⁾ Among these kinetic equations, the best linearity was found with the Avrami-Erofe'ev equation (A₂). The data plotted in this manner are shown in Fig. 9 ($0.2 \leq \alpha \leq 0.9$). This result suggests that the dehydration reaction proceeds by random nucleation of the product followed by two-dimensional growth of nuclei.

The progress of dehydration was continuously observed

Fig. 9. Isothermal Dehydration of Theophylline Hydrate Evaluated According to the Avrami-Erofe'ev Equation (A₂)

●, 47.2°C; ●, 49.0°C; ⊖, 51.0°C; ○, 53.2°C.

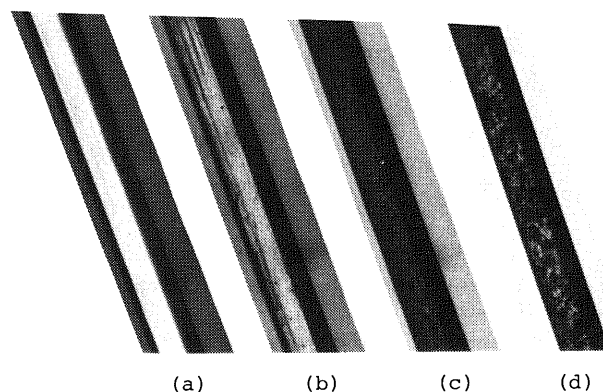
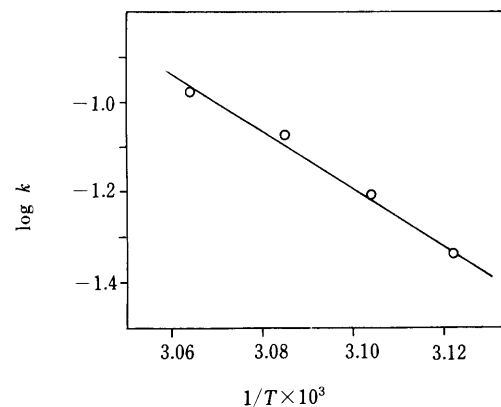


Fig. 10. Dehydration Process of a Crystal of Theophylline Hydrate in Air at 48°C

(a) Room temperature. (b) After 10 min at 48°C. (c) After 20 min at 48°C. (d) After 25 min at 48°C.

Fig. 11. Temperature Dependence of k for the Isothermal Dehydration of Theophylline Hydrate

under a microscope. As shown in Fig. 10, after 10 min at 48°C, black points, growing nuclei of dehydrated theophylline, appear sporadically. After 20 min, the nuclei increase in number and spread all over the surface of the crystal. The area occupied by the product increases two-dimensionally and the dehydration reaction proceeds vigorously. After 25 min, the reaction had proceeded further. Thus, microscopic observations were well consistent with the kinetic studies.

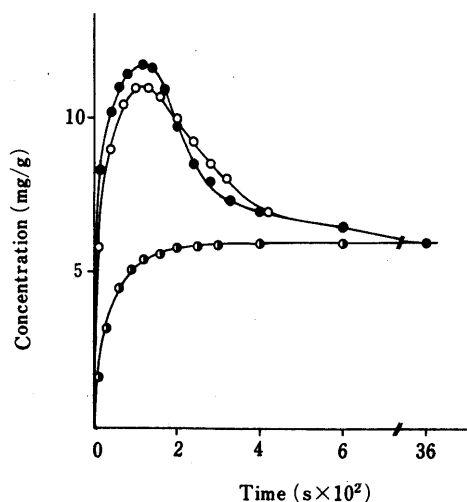


Fig. 12. Dissolution Curves of Theophylline at 25°C in Water
●, anhydrous form II; ○, anhydrous form I; ◐, hydrate.

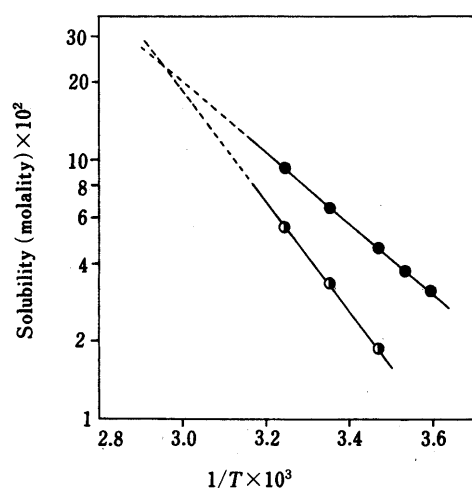


Fig. 13. The van't Hoff Plots of Solubility Values for Anhydrous Theophylline Form II and Hydrate
●, anhydrous form II; ◐, hydrate.

In contrast to our data, Shefter *et al.* have reported that the hydrate transforms to an anhydrous form with apparent zero-order kinetics.¹¹⁾ Since they used ground crystals of the hydrate, different results would be expected.¹²⁾

From the slopes of the straight lines in Fig. 9, the values of the dehydration rate constants, k , were evaluated. Increases in reaction rate with temperature are often found to obey the Arrhenius equation. Figure 11 shows the linear re-

lationship between $\log k$ and $1/T$. From the slope the activation energy of dehydration was calculated to be 120 kJ/mol.

Dissolution of Theophylline and Its Hydrate As seen in Fig. 12, the two anhydrous forms dissolve much faster than the hydrate and yield concentrations substantially supersaturated with respect to the stable form. Shefter and Higuchi reported the dissolution behavior of crystalline hydrates of some pharmaceuticals.¹³⁾ They stated that the maximum values observed in dissolution curves may correspond to the solubility of the anhydrous crystalline phase or represent a short-term steady-state phase situation involving equal rates of dissolution of the metastable form and crystallization of the stable hydrate.

IR spectra of the solid residue in the dissolution medium demonstrate that rapid transformation from the anhydrous form to the hydrate occurs immediately after the beginning of the experiments. Anhydrous form I transformed more easily, and therefore, a reliable approximation of the solubility could not be obtained. Measurements of anhydrous form II over the temperature range of 5 to 45°C, when plotted in the van't Hoff fashion, give a good linear relationship as shown in Fig. 13. The data for the stable hydrate are also given in the same figure. These two lines intersected at 66.0°C and this value agreed very well with the stability point of the hydrate ($67.0 \pm 0.2^\circ\text{C}$) reported by Bruns *et al.*²⁾

References and Notes

- 1) E. Suzuki, K. Shirohani, Y. Tsuda, and K. Sekiguchi, *Chem. Pharm. Bull.*, **33**, 5028 (1985).
- 2) S. Bruns, J. Reichelt, and H. K. Cammenga, *Thermochim. Acta*, **72**, 31 (1984).
- 3) A. Burger and R. Ramberger, *Microchim. Acta*, **1979** II, 273.
- 4) G. Spittler and M. Spittler-Friedman, *Monatsh. Chem.*, **93**, 632 (1962).
- 5) H. Doser, *Arch. Pharm.*, **281**, 251 (1943).
- 6) D. J. Sutor, *Acta Crystallogr.*, **11**, 83 (1958).
- 7) D. A. Wadke and G. E. Reier, *J. Pharm. Sci.*, **61**, 868 (1972).
- 8) The normal maximum and minimum relative humidities are the average values of the last three decades (1951–1980).
- 9) Tokyo Astronomical Observatory (ed.), "Chronological Scientific Tables," Maruzen Co., Ltd., Tokyo, 1988, p. 207.
- 10) J. H. Sharp, G. W. Brindley, and B. N. Narahari Achar, *J. Am. Ceram. Soc.*, **49**, 379 (1966); C. H. Bamford and C. H. F. Tipper (ed.), "Reactions in the Solid State, Comprehensive Chemical Kinetics," Vol. 22, Elsevier Scientific Publishing Company, Amsterdam, 1980, Chapter 3.
- 11) E. Shefter, H. Fung, and O. Mok, *J. Pharm. Sci.*, **62**, 791 (1973).
- 12) K. Sekiguchi, K. Shirohani, O. Sakata, and E. Suzuki, *Chem. Pharm. Bull.*, **32**, 1558 (1984).
- 13) E. Shefter and T. Higuchi, *J. Pharm. Sci.*, **52**, 781 (1963).